



Anthocyanin modified by chondroitin sulphate and tannic acid improved the quality-indicating properties of gelatin-based intelligent film

Ruoyi Hao^{a,*}, Shiwen Pang^b, Jan Mraz^c, Yeye Geng^a, Yanqiu Liu^a, Jinfeng Pan^{b,*}

^a Department of Food Science and Technology, School of Forestry, Beihua University, Jilin 132013, China

^b National Engineering Research Center for Seafood, Collaborative Innovation Center of Provincial and Ministerial Co-construction for Seafood Deep Processing, Liaoning Province Collaborative Innovation Center for Marine Food Deep Processing, Dalian Polytechnic University, Dalian 116034, China

^c The University of South Bohemia in Ceske Budejovice, Faculty of Fisheries and Protection of Waters, Institute of Aquaculture and Protection of Waters, Ceske Budejovice 37005, Czech Republic

ARTICLE INFO

Keywords:

Anthocyanin
pH-sensitive film
Co-pigmentation
Enhanced recognition accuracy
Sub-freshness monitoring

ABSTRACT

A highly pH-responsive gelatin film incorporating purple cabbage anthocyanin (PCA) and chondroitin sulphate (CS)/tannic acid (TA) was developed. Co-pigmentation of PCA via CS/TA improved its photothermal stability and visibility of color change in gelatin film. The morphological and structural properties of CS-PCA and TA-PCA films revealed that a more stable network was formed as new hydrogen bonds were generated by the co-pigmentation. Meanwhile, the co-pigmentation improved film's mechanical and hydrophobic properties, expressed as higher tensile strength (16.65 and 17.97 Mpa) and lower water vapor permeability (1.45 and 1.41) in CS-PCA and TA-PCA films, compared to PCA film. CS-PCA and TA-PCA films showed distinct color transitions for chilled fish fillets during storage. Total color difference (ΔE) of CS-PCA and TA-PCA films correlated well with the deterioration indexes of total volatile base nitrogen (TVB-N). All the results provided a novel pH-sensitive intelligent packaging strategy by co-pigmenting CS/TA with PCA for freshness monitoring.

1. Introduction

With increased knowledge of food quality and safety, consumers expect food packaging to be multifunctional in addition to preservation, such as more intuitive, timely and rapid feedback, and identification of food deterioration (Xu et al., 2024). Intelligent film, which could monitor environmental changes or specific compounds generated during food storage and give information of food freshness via real-time signals readable by naked eye to consumers, has received growing interest. The pH inside the packaging could be modified by the changes in concentration of organic acids and volatile compounds (e.g., volatile nitrogen, ammonia metabolites, etc.) as a result of microorganism growth and metabolism during food spoilage (R. Hao et al., 2017). Thus, the quality of food might be converted into a real-time visual message for the consumer, a color shift, by incorporating pH-sensitive indicators into packaging material to perceive pH change dynamically.

Considering food safety and quality, pH-sensitive indicators from natural pigments could be more acceptable than synthetic ones. Anthocyanins are a group of natural water-soluble pigments present in a wide variety of fruits and vegetables. Due to their ability to sense pH

visually and biosafety, anthocyanins are frequently utilized as natural indicator in intelligent films for denoting food freshness. Researches on films prepared from chitosan (Tavassoli, Khezerlou, Firoozy, Ehsani, & Punia Bangar, 2023), chitosan/chitin nanofibers (Wang et al., 2023), chitosan/gelatin (Li, Wang, Feng, Zhuang, & Zhu, 2024) and carboxymethyl cellulose/gelatin bio-nanocomposite (Sadi & Ferfera-Harrar, 2023) had demonstrated that the anthocyanins enhanced the chemical and physical characteristics of films, and they demonstrated notable color changes when foods were spoiled. However, anthocyanins are susceptible to environmental factors, such as oxygen, light, temperature, metal ions, etc., which would weaken the colorimetric monitoring function and interfere with the assessment of food freshness. Thus, how to improve the stability of anthocyanin used in film becomes a main problem in developing an intelligent film.

Strategies including molecular co-pigmentation, structural modification and microencapsulation have been tried to stabilize anthocyanin. Among them, co-pigmentation is the commonest one. The co-pigmentation phenomenon takes place when pigment (anthocyanins) and co-pigment (colorless substance, e.g. polysaccharides, proteins, amino acids and ions) form non-covalent, preventing flavonoid cations

* Corresponding authors.

E-mail address: ruoyiHAO@beihua.edu.cn (R. Hao).

<https://doi.org/10.1016/j.fochx.2024.101779>

Received 12 June 2024; Received in revised form 22 August 2024; Accepted 24 August 2024

Available online 26 August 2024

2590-1575/© 2024 Published by Elsevier Ltd. This is an open access article under the CC BY-NC-ND license (<http://creativecommons.org/licenses/by-nc-nd/4.0/>).

from hydrophilic nucleophilic attack (Huang et al., 2023). This could cause a wavelength shift of the maximum absorbance toward higher values (bathochromic shift) and an increase in visible absorbance (hyperchromic shift). These changes could stabilize and modulate the color of anthocyanin, resulting in a more vibrant, intense, and sharp color than anthocyanin alone.

Phenolic acids could be effective copigments for anthocyanin since they play a key role in preventing the loss of anthocyanins in a variety of fruits and vegetables (S. Liu et al., 2019a). Tannic acid (TA) has 25 hydrogen bond donors, which is possible to form many intermolecular hydrogen bonds with anthocyanin. Thus, it could be a good co-pigment candidate. Chondroitin sulphate (CS) is an acidic mucopolysaccharide with a negative charge, which can interact with anthocyanin to form π - π stacking for allowing intermolecular stacking to enhance the chromaticity of anthocyanin (Tan, Selig, & Abbaspourrad, 2018). Moreover, through hydrogen bonding, TA and CS can form a stable cross-linked network with various film matrices such as gelatin or polysaccharide, which may physically encapsulate anthocyanins to protect them. Based on these hypotheses above, binding TA or CS to anthocyanin might enhance the color sharpness and improve the stability of the natural pigment. Although co-pigments have been used progressively in the beverage and pigment extraction industries (S. Liu et al., 2019a), their use in intelligent colorimetric packaging films is scarcely reported.

Our previous study showed the incorporation of purple cabbage anthocyanin (PCA) under the aid of ultrasound improved the mechanical properties and water resistance of gelatin-oil intelligent film (Pang et al., 2023). The purpose of this study mainly to enhance the stability and color intensity of PCA through co-pigmentation with CS and TA, so as to provide better freshness-indicating function to intelligent film using PCA as indicator. The morphologic, mechanical and structural properties of films were characterized along with antioxidative capacity, color reactions and storage stability of films. The films were applied for real-time quality-monitoring of fish muscle as well.

2. Materials and methods

2.1. Chemicals and materials

CS and TA were purchased from Macklin Co., LTD. (Shanghai, China). Purple cabbage powder was produced by Hebei Kangan Medicine Co., LTD. (Hebei, China). Fresh carp was bought from Meilinyuan Agroproduct Market (Dalian, China). All the other chemicals were of analytical grade and purchased from Sangon Biotech Co., LTD. (Shanghai, China). Detailed information about all chemicals and reagents, including catalog number, manufacturer, city, and country is listed in Table S1.

2.2. PCA extraction and modification

Solvent extraction method was used to extract PCA from purple cabbage powder, according to Pang et al. (2023). Briefly, the powders were mixed at a solid-liquid ratio of 1:20 with 75 % ethanol: 1 % citric acid (1:1, v/v), and performed in a 60 °C water bath for 3 h. The extracted solution was then centrifuged at 8000g for 10 min. The collected supernatant was freeze-dried as PCA. To obtain modified PCAs, PCA water solution (140 mg/mL) was mixed with CS (5 mg/mL) or TA (17 mg/mL) water solution at a volume ratio of 1:1. The combinations were magnetically stirred for 3 h at room temperature. The modified PCAs were named as CS-PCA and TA-PCA, respectively.

2.3. Characterization for modified PCA solutions

2.3.1. pH-sensitivity

Color-changing and pH-sensitivity of PCA and modified PCA solutions were tested by adjusting them into various pH values (2.0–12.0) via the buffer solutions (citric acid and disodium phosphate). A smart

phone camera was used to take picture of those tested solutions. An UV-Vis Spectrophotometer (Lambda35, Perkin Elmer, Madison, USA) was used to measure their UV-vis spectra. The scanning wavenumber was 400–800 nm.

2.3.2. Fourier transforms infrared (FTIR) spectra

PCA and modified PCA solutions at various pH values (2.0–12.0) were scanned by an FTIR spectrometer (Spectrum II Frontier, Perkin Elmer, LTD., Massachusetts, USA) under attenuated total reflectance mode (resolution 4 cm^{-1}) in the spectral range of 500–4000 cm^{-1} to evaluate the chemical interactions between PCA and copigments (CS and TA).

2.4. Film preparation

Films were prepared by previous method with modifications (Pang et al., 2023). A mixture with 5 % gelatin (m/v), 5 % sunflower oil (v/v), 3 % glycerol (v/v), and 0.1 % tween-80 (v/v) was prepared. The mixture was continuously stirred for 2 h at 60 °C to obtain homogeneous solution. PCA or CS-PCA or TA-PCA (4 %, v/v) was mixed into the solution in a beaker, homogenized and ultrasonicated by a Probe Ultrasonic Apparatus (PART NO. 630–0219, Sonics & Materials, Newtown, USA) at 600 W for 10 min (2 s off and 2 s on) to obtain the film-forming solution. The beaker was kept in cool water during this period. The film solution was cast into a Petri dish and dried in an incubator for 24 h at 25 °C. All films were equilibrated in a chamber with 50 % humidity for 24 h, and then peeled off for testing.

2.5. Film characterization

2.5.1. Structural and morphological properties

An FTIR spectrometer (Spectrum II Frontier, PerkinElmer, Massachusetts, USA) was used to analyze the bonding types among molecules of PCA or CS-PCA or TA-PCA films matrix with the spectral range of 500–4000 cm^{-1} under attenuated total reflectance mode (resolution 4 cm^{-1}) (Ebrahimi Tirtashi et al., 2019). A XRD Diffractometer (XRD6100, Shimadzu, Tokyo, Japan) was used to evaluate the crystal phase of film in the 2θ range of 5–40° with a 5°/min scanning rate at RT (Nam, French, Condon, & Concha, 2016).

The morphology of cross-section and surface of film was observed by using a Scanning Electronic Microscopy (SEM) (JSM-7800F, JEOL, Tokyo, Japan) with accelerating voltage of 15 kV. Before analysis, a small piece of film was frozen in liquid nitrogen, broken naturally and sputtered with gold-palladium by a Sputter Coater (SCD005, Ba-Tec Co., Tettngang, Germany).

2.5.2. Differential scanning calorimetry (DSC) analysis

Film (10 mg) was placed into an aluminum pan, and hermetically sealed. A DSC (TA-DSC-250, TA instruments, New Castle, USA) was applied to analyze the thermal characteristics in a temperature range of 20–100 °C with a 5 °C/min raising rate.

2.5.3. Physical properties analysis

Film thickness was measured using a Digital Micrometer (QNIX4500, AICE, Taizhou, China) (accuracy = 0.001 mm). Thicknesses of five random spots of each film (40 mm × 40 mm) were measured, and the average value was calculated as final film thickness.

Tensile testing was performed via a texture analyzer (TA. XT Plus, SMS, Surrey, UK) as (Pang et al., 2023) to determine tensile strength (TS) and elongation at break (EB). Briefly, film strip (60 mm × 10 mm) was fixed and deformed with crosshead stretching speed of 60 mm/min until broken. TS (MPa) was calculated as below:

$$TS = F^m / L \times W \quad (1)$$

where L was the beginning stretching distance (mm), W was the film

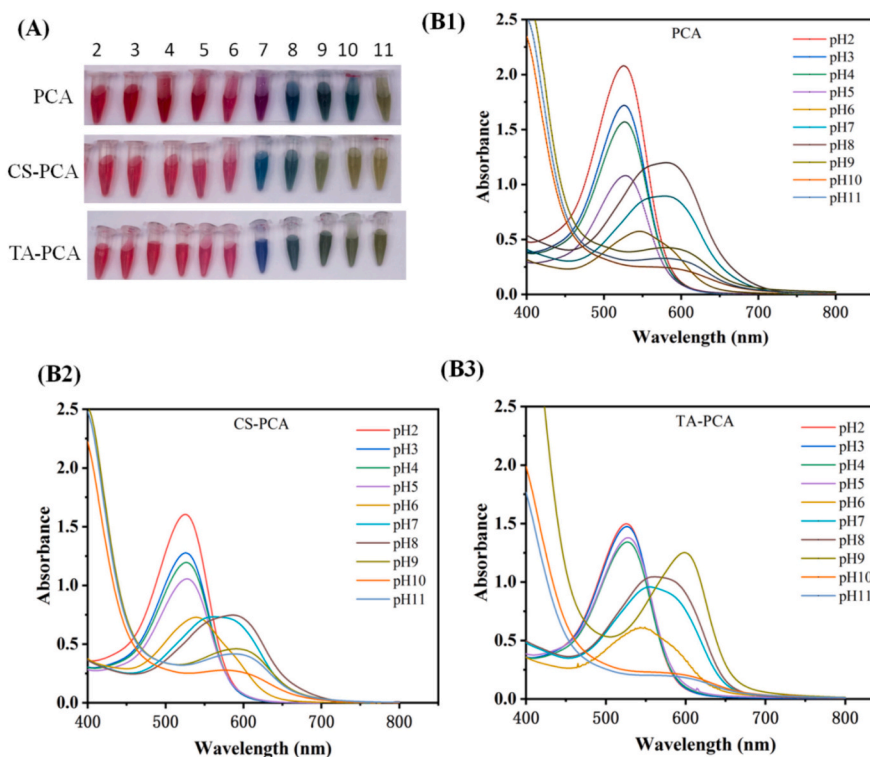


Fig. 1. Color (A) and UV-vis spectra of purple cabbage anthocyanin (PCA) (B1), PCA modified by chondroitin sulphate (CS-PCA) (B2) and tannic acid (TA-PCA) (B3) at pH 2–11. (For interpretation of the references to color in this figure legend, the reader is referred to the web version of this article.)

thickness (mm), and F_m was the maximum value of axial tension on the material specimen (N).

EB was calculated as below:

$$EB (\%) = \frac{L_1 - L_0}{L_0} \times 100\% \quad (2)$$

where L_1 was the final stretching distance (mm), and L_0 was the starting of the stretching distance (mm).

The transmittance of visible light through films was measured using an UV-visible Spectrophotometer (Lambda 35, Perkin Elmer., Madison, USA) at wavelength 400–800 nm. Film opacity was calculated using the formula:

$$\text{Opacity (A mm}^{-1}\text{)} = \frac{A}{X} \quad (3)$$

where X was the film thickness (mm) and A was the film absorbance under 600 nm.

Water vapor permeability (WVP) of film was evaluated using ASTM E96–05 method as Li, Wang, et al. (2024) with modifications. Film (50 mm × 50 mm) was sealed over a glass cup (diameter 40 mm, depth 25 mm) with 10 g anhydrous CaCl_2 inside, and kept in a desiccator (25 °C, 90 % RH) set by a saturated KCl solution. The glass cup was continuously weighed each 2 h during 24 h. WVP (g mm/Pa cm^2 h) was calculated using the formula:

$$WVP = \frac{WVTR \times L}{\Delta P} \quad (4)$$

where L was film thickness (mm), ΔP was water vapor pressure differential (Pa) between the two sides of the film, and WVTR was the water vapor transmission rate, which is calculated by dividing the slope of the straight line by the exposed film area (cm^2).

Wettability of film was analyzed as water contact angle (WCA) using a Drop Shape Analyzer (DSA25, Kruss, Hamburg, Germany) as our

pervious method (Pang et al., 2023). Briefly, film (20 mm × 20 mm) were positioned and secured on a horizontal movable stage. WCA was determined immediately after applying a 5 μL droplet of distilled water onto the film surface. A Charged Coupled Device camera recorded the instantaneous image of the drop, and WCA was calculated using attached software.

2.6. Antioxidative activity of film

A DPPH method was used to measure the antioxidative activity of film according to (Pang et al., 2023). Briefly, film was dissolved in 95 % ethanol and the supernatant was reacted with DPPH-ethanol solution. The film's absorbance at 517 nm was measured using a Microplate Reader (Infinite M200, Tecan, Mannedorf, Switzerland), and the DPPH radical scavenging capacity was computed. Antioxidant activity of the film was calculated as a percentage of its ability to scavenge DPPH radicals:

$$\text{DPPH radical scavenging activity (\%)} = \frac{(A_0 - A_s)}{A_0} \quad (5)$$

where A_0 was absorbance at 517 nm of DPPH and A_s was absorbance at 517 nm of film solution.

2.7. Film color response to pH

Film (40 mm × 40 mm) was soaked into various buffer solutions (5 mL, in a pH range 2.0–12.0) for 5 min at room temperature. A digital camera was used to capture color response in natural light. The color parameters (i.e. L^* , a^* , and b^*) of film were measured using a Colorimeter (UltraScanPro, Hunter Lab Inc., Reston, USA). The total color difference (ΔE) was calculated as the following formula:

$$\Delta E = \sqrt{(L - L_w)^2 + (a^* - a_w^*)^2 + (b - b_w)^2} \quad (6)$$

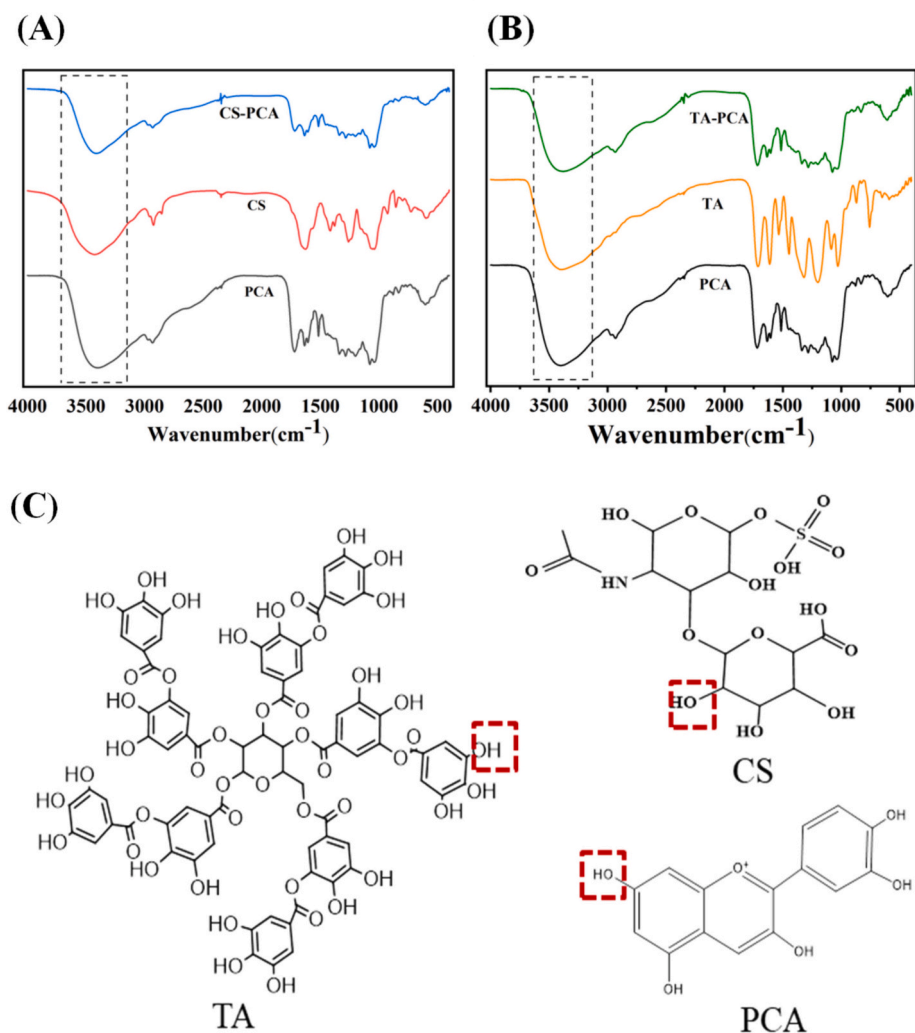


Fig. 2. FT-IR spectra of PCA, CS, CS-PCA (A), PCA, TA, TA-PCA (B) and possible interactions between CS or TA and PCA (C). Abbreviations see Fig. 1.

where L_w , a_w^* , b_w were the standard value of the white plate, and L , a^* , b were the measured value of film sample. L represents lightness, or how bright or dark a color is. The value a^* represents the red-green, with negative values representing green and positive values representing red. The value b represents the blue-yellow, with negative values representing blue and positive values representing yellow.

2.8. Film stability

Film PCA, CS-PCA and TA-PCA were kept at 25 °C in both light and dark conditions for 14 days to investigate their stability. Color parameters (L , a^* , and b) of film were recorded by a Colorimeter (UltraScanPro, Hunter Lab Inc., Reston, USA) every 2 days. ΔE value was calculated as

$$\Delta E = \sqrt{(L - L_0)^2 + (a^* - a_0^*)^2 + (b - b_0)^2} \quad (7)$$

where L_0 , a_0^* , b_0 were the standard value of film on 0 day, and L , a^* , b were the measured value of film sample.

2.9. Monitoring test of fish spoilage by films

Approximately 10 g fresh fish fillets were put into sterilized plastic petri dishes and packed with film PCA, CS-PCA and TA-PCA, respectively. They were stored at 4 °C for 8 days to check the quality-

monitoring function of films. pH value of fish fillet was measured using a digital pH meter (PHS-3C, INESA Scientific Instrument Co., Shanghai, China) as R. Y. Hao, Pan, Khalili Tilami, Shah, and Mráz (2020). TVBN (mg/100 g) of the fish was determined as R. Hao et al. (2017). Briefly, minced sample was stirred in deionized water (1:10, m/v) for 30 min, and the filtrate was mixed with the saturated K_2CO_3 (1:1 v/v). The mixture was incubated in Conway's dish at 37 °C for 2 h with a boric acid solution (20 g/L) with methyl red-methylene blue indicator (2 g/L). The TVBN value was calculated by the titration volume of a 0.01 M HCl standard solution. Film color changes during storage were recorded by a digital camera and determined by a Colorimeter (UltraScanPro, Hunter Lab Inc., Reston, USA) as Section 2.7. The correlations between color properties and pH or TVBN were studied to evaluate the monitoring roles of films.

2.10. Statistical analysis

Experiment was triplicated, and the results were presented as mean \pm standard deviation (STD). Statistical analysis of the data was carried out using IBM SPSS Statistics software 19.0 (SPSS Inc., Chicago, IL, USA). One-way analysis of variance (ANOVA) was performed, and the differences between groups were assessed via Duncan's multiple range test. A significant different level of $p < 0.05$ was set.

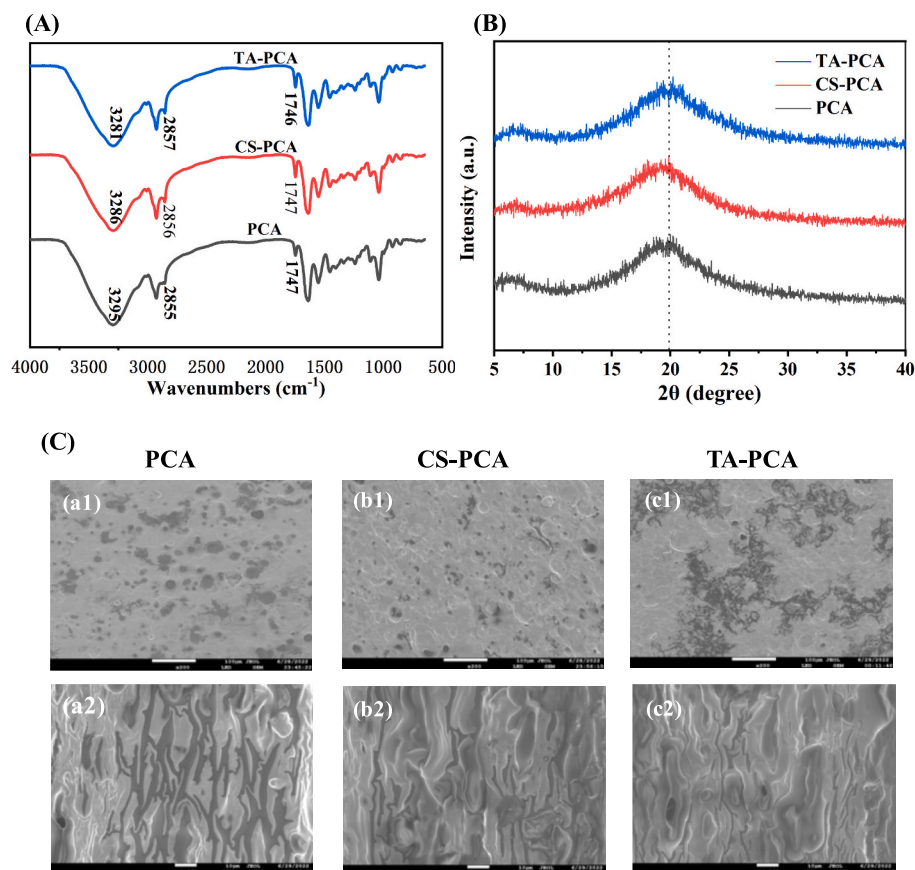


Fig. 3. FT-IR spectra (A), XRD pattern (B) and SEM micrographs (C) of surface (200 \times , a1-c1) and cross-section (1000 \times , a2-c2) of PCA, CS-PCA, TA-PCA films. Abbreviations see Fig. 1.

3. Results and discussion

3.1. Color and UV-vis spectral of modified PCAs

UV-vis spectra and color change of PCA, CS-PCA and TA-PCA solutions in the pH range of 2.0–12.0 were shown in Fig. 1. As demonstrated in Fig. 1A, PCA solution was red-pink in pH 2–6 with a tendency turning light, which was attributed to the structural change from flavin cations to carbinol pseudo base (Tang et al., 2019). Color change from red to pink under pH 2–6 was also reported in carrot anthocyanins by Ebrahimi Tirtashi et al. (2019). The color of PCA was purple at pH 7, and blue-green in a range of pH 8–10, while appeared as green-yellow at pH 11, which coincided with the color change of roselle anthocyanin under pH 7–12: violet, pH = 7; blue/green to green, pH 8–10; yellow, pH = 12) (Sadi & Ferfera-Harrar, 2023). The color changes under pH 7–12 might due to the presence of quinoidal base and chalcone (Tang et al., 2019). The color of CS-PCA and TA-PCA exhibited similar change with PCA. However, their turn more light in pH 2–6. Unlike PCA appeared purple, color of CS-PCA and TA-PCA turned blue directly at pH 7, which enhanced the contrast between pH 6 and pH 7, which is a key pH range for fish quality. Chenjing Xie, Ying, Wang, Wang, and Huang (2020) observed similar result. Above results indicated that the copigmentation by CS and TA could to boost anthocyanins color change (Susanti, Wijaya, Hasanah, & Heryani, 2018).

The UV-vis spectra of PCA, CS-PCA and TA-PCA solutions under different pH value are illustrated in Fig. 1B1–B3. All PCA spectra curve showed a single peak which was shifted from 525 nm to 595 nm. The peak shifting agreed with their color changes from red to green. It is noticed that the maximum absorption peak of TA-PCA and CS-PCA moved to long wavelength at pH 7–8 compared to PCA, which could be due to the strong interactions between the copigments and PCA,

leading to the changes in absorption intensity and displacement (You et al., 2019). Similar results were found in blueberry anthocyanins copigmented with CS (Bao et al., 2022) and roselle anthocyanin copigmented with oxalic acid (Huang et al., 2023). Above indicates that PCA was modified by CS and TA, and the modifications might provide better pH-responsive color change for improving its function as intelligent film indicator.

3.2. FTIR spectra of modified PCAs

Several insights into the molecular interactions between PCA and copigments (TA and CS) were showed by FTIR spectrum (Fig. 2A-B). The FTIR spectrum of PCA showed characteristic bands at 1720 cm^{-1} (C=O stretching vibration), 1635 cm^{-1} (C–C stretching vibration), 1605 cm^{-1} (C=C stretching vibration), 1073 cm^{-1} (C–H deformation), and 3400 cm^{-1} (O–H stretching vibration) and 2931 cm^{-1} (C–H stretching vibration) (Liang, Sun, Cao, Li, & Wang, 2019; Y. Wang, Zhang, & Zhang, 2022). CS-PCA spectra showed similar peak pattern with that of PCA. However, The O–H band peak was shifted from 3400 to 3412 cm^{-1} , suggesting the formation of hydrogen bonds between CS and PCA. Further, bands at 1720 and 1073 cm^{-1} was shifted to 1718 and 1077 cm^{-1} , respectively, implying the introduction of hydroxyl groups might promote C=O stretching vibration. When comes to TA-PCA spectra, the peak of O–H band moved from 3400 to 3386 cm^{-1} with enhanced intensity, suggesting the formation of additional hydrogen bonds between TA and PCA. Moreover, shifting peaks appeared at 2935 cm^{-1} (C–H stretching vibration), 1718 cm^{-1} (C=O stretching vibration), and 1076 cm^{-1} (C–H deformation of aromatic ring), which could result from the formation of intermolecular hydrogen bonds between PCA and TA (Susanti et al., 2018). It's known that TA molecule contains 25 hydrogen bond donors that could form many hydrogen bonds with anthocyanins

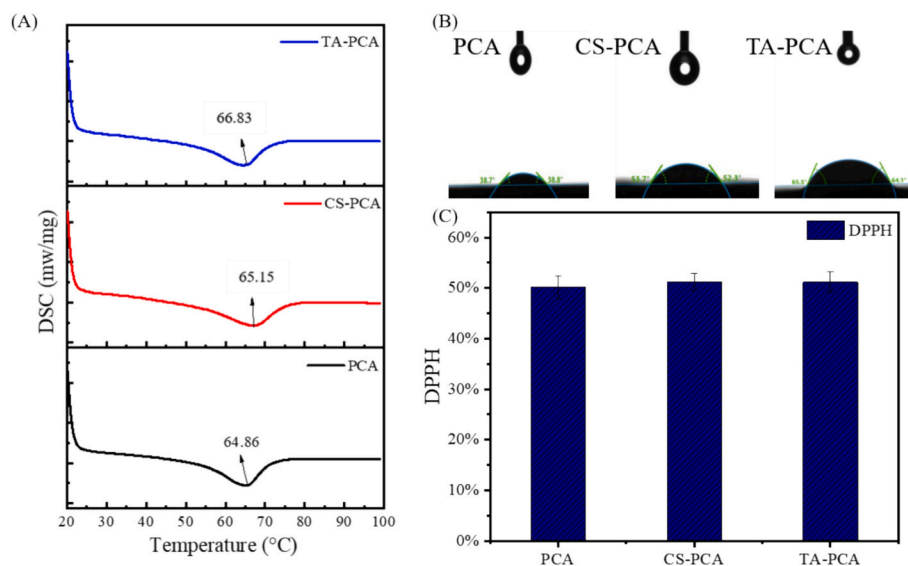


Fig. 4. DSC analysis (A), water contact angle images (B) and DPPH radical scavenging activity (C) of PCA, CS-PCA, TA-PCA films. Abbreviations see Fig. 1.

molecules (Fig. 2C) (Baldwin & Booth, 2022).

3.3. Film characteristics

3.3.1. Morphology and structure analysis

The FT-IR spectra of PCA, CS-PCA and TA-PCA films are shown in Fig. 3A. The C=O stretching of amide-I, N-H bending of amide-II, and C-N & N-H stretching of amide-III were detected at 1747, 1552 and 1236 cm^{-1} , respectively, in PCA films, which are the characteristic bands of gelatin-based film (Sadi & Ferfera-Harrar, 2023). Similar peaks patterns were observed in PCA, CS-PCA and TA-PCA films, except O-H stretching moved from 3295 to 3286, 3281 cm^{-1} , respectively, together with the stronger intensity. It implying more hydrogen bonds might be formed between CS/TA and PCA. No obvious shift or alteration in peak intensity and positions of three films suggests no significant chemical modifications within the composite films, implying only physical interactions, like hydrogen bonding and van der Waals forces, occurred among gelatin, PCA and CS/TA (Riahi, Khan, Rhim, Shin, & Kim, 2023). This result is consistent with the findings of potato starch-based intelligent film containing blueberry anthocyanin and chondroitin sulphate (Bao et al., 2022) and gelatin-based intelligent film incorporated with rosele anthocyanin and oxalic acid (Huang et al., 2023).

XRD analysis was done to shed some lights on the physical condition of films. As depicted in Fig. 3B, XRD patterns of all films revealed peaks around $2\theta = 6-7^\circ$ and $2\theta = 19-20^\circ$, which were associated with triple helix diameter and crystallinity of the gelatin, respectively (Pan et al., 2020). Similar peaks patterns were reported in an anthocyanin-loaded gelatin film by Etxabide, Maté, and Kilmartin (2021) and a CMC/Gelatin bio-nanocomposite films with red cabbage anthocyanins by Sadi and Ferfera-Harrar (2023). CS-PCA and TA-PCA had little effect on the reordering of the gelatin crystalline region in gelatin-based PCA film, which indicates that the addition of CS and TA did not affect the original crystal structure of PCA film. This was also reported in a chitosan/

gelatin film loaded with black peanut seed coat anthocyanin (BPSCA), which found no effect on the original crystal structure of chitosan/gelatin film (Lu, Zhou, Yu, Chen, & Yuan, 2022).

SEM was used to investigate the potential effect of modified PCAs on microstructure of the films. The surfaces of all films were uniform and smooth (Fig. 3C, a1-c1), indicating the successful compatibility between PCA/CS-PCA/TA-PCA and gelatin. It is consistent with the finding that anthocyanins were generally well dispersed in sodium alginate/gelatin get along well (Chen et al., 2023). The cross sections of all three films were relatively homogenous (Fig. 3C, a2-c2). Compared with PCA film, slightly increasing compactness was found in film CS-PCA and TA-PCA, indicating the co-pigmentation of PCA with CS/TA might have slightly positive influence on film structure. This could be explained by the formation of new hydrogen bonds between CS/TA and PCA, which help PCA and gelatin better form dense cross-linked network. This is consistent with the results by FTIR. A more homogeneous surface in a PVA/HPMC film incorporating rosele anthocyanin co-pigmented with oxalic acid was reported by Huang et al. (2023). It's considered that by preventing anthocyanin degradation, precipitation and movement, PCA co-pigmented by oxalic acid could stabilize the micro-structural network of film.

3.3.2. Thermal property

In Fig. 4A, all films had a single endothermic peak, which suggests a good compatibility among all components in the film. This is consistent with SEM results. The melting temperature of film CS-PCA and TA-PCA showed slightly increase (65.15 °C and 66.83 °C) compared to film PCA (64.86 °C). This indicates that adding CS-PCA and TA-PCA might increase the thermal stability of film. This could be associated with the hydrogen bonding and electrostatic attractions among CS/TA, PCA and gelatin, which was also supported by FTIR results. Similarly, Kang et al. (2020) reported the increase of the melting temperature of film due to the formation of hydrogen bonds between rose anthocyanins and okra

Table 1
Physical properties of films.

Film	Thickness (mm)	TS (Mpa)	EB (%)	Opacity	WVP ($\text{g}\cdot\text{mm}/(\text{m}^2\cdot\text{h}\cdot\text{kPa})$)
PCA	0.078 ± 0.008^a	14.43 ± 0.89^a	50.89 ± 7.35^a	3.37 ± 0.90^a	1.69 ± 0.12^a
CS-PCA	0.074 ± 0.005^a	16.65 ± 1.41^{ab}	67.46 ± 8.29^b	3.31 ± 0.51^a	1.45 ± 0.08^b
TA-PCA	0.073 ± 0.007^a	17.97 ± 1.77^b	69.83 ± 7.64^b	3.40 ± 0.07^a	1.41 ± 0.09^b

Low case letters in each row are significantly different ($p < 0.05$).

TS: tensile strength, EB: elongation at break, WVP: water vapor permeability.

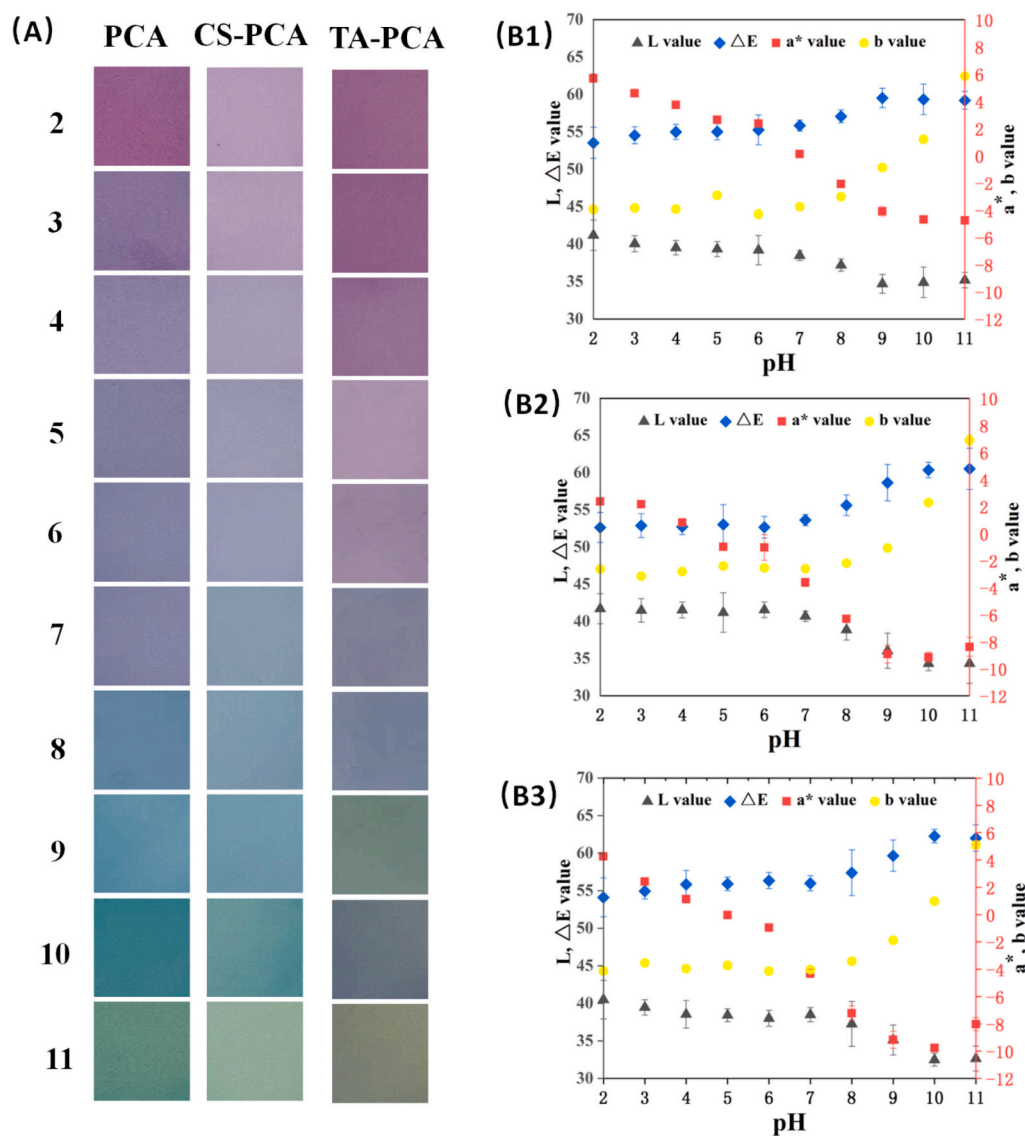


Fig. 5. The color response (A) and color properties (B1-B3) of PCA, CS-PCA and TA-PCA films to different pH buffer solutions. PCA, CS-PCA and TA-PCA films are films using PCA, CS-PCA and TA-PCA as indicator. Abbreviations see Fig. 1.

mucilage polysaccharide.

3.3.3. Physical properties and anti-oxidative activity

Thickness directly affect the film's mechanical strength, light transmittance, and water vapor permeability, and opacity could affect the quality of food packaging since the nutrients and bioactive ingredients in food may oxidize and degrade under the strong light. In Table 1, no significant variation in film thickness and opacity was observed among film PCA, CS-PCA and TA-PCA, indicating the co-pigmentation of PCA with CS/ TA have no big effects on thickness and opacity. Thickness and opacity of film depends mainly on the composition of films, and the addition of CS/TA in low dose showed no effect on the composition of film.

WVP is a crucial metric of the applicability of food packaging. One of the main purposes of food packaging film is to prevent or reduce moisture transmission from the food to the environment. In Table 1, the water resistance of film was improved by CS-PCA and TA-PCA, as evidenced by their WVP values of 1.45 and 1.41 g mm/m⁻² h kPa, respectively, which were lower than the WVP of PCA film (1.69 g mm/m⁻² h kPa). As demonstrated by FT-IR analysis, the development of crosslinking between the CS/TA and PCA via hydrogen bonds might

explain the enhanced water resistance of film CS-PCA and TA-PCA. It is in line with the findings reported by Huang et al. (2023), who stated that incorporating roselle anthocyanin together with oxalic acid into the film could improve water barrier capability via new hydrogen bonds formed during co-pigmentation. Similarly, Li, Feng, Wang, Zhuang, and Zhu (2024) also observed the reduction on WVP of the sodium alginate/carrageenan polysaccharide film incorporating bilberry anthocyanins as indicator and tannin acids as co-pigment. It's considered that these interactions would lower the free volume of polymer matrix, resulting in the development of a more compact film network and enhanced defense against the penetration of water vapor (Zhao et al., 2022).

The surface hydrophilicity and wettability of the composite films were examined by WCA. All three films showed a WCA lower than 90°, indicating hydrophilic surface characteristics (Fig. 4B). The higher the angle, the lower the wettability, and the higher hydrophobic performance of the material. By through co-pigmentation with CS or TA, the WCA of film PCA (38.8°) increased significantly ($p < 0.05$) (film CS-PCA 53°, film TA-PCA 64.8°), indicating the decreased hydrophilicity of film surface (consistent with the results in WVP). These findings could be explained by the formation of new hydrogen bonds between CS/TA and PCA, which reduced the binding to water molecules and created a more

condensed structure, resulting in a more hydrophobicity film surfaces (Qin et al., 2021) (in agreement with the FTIR and SEM results). Similar results were found in CMC/gelatin based film integrated with red cabbage anthocyanins after adding pistacia leaves extract (PE), in which the phenolic compounds of PE and the film matrix compounds may interact powerfully via forming hydrogen bonds and form a more compact structure (Sadi & Ferfera-Harrar, 2023). Moreover, the large amount of aromatic polar groups present in TA might also affected WCA, which supported by Wang, Xie, et al. (2023), who reported a high WCA in chitosan/esterified chitin based film loaded eggplant peel anthocyanins. However, in opposition to our findings, Li, Feng, et al. (2024) have reported that the addition of bilberry anthocyanins and tannin acids in sodium alginate/carrageenan polysaccharide based films showed a decreased WCA.

Tensile strength (TS) shows the film's maximal ability to withstand damage under static tensile conditions, which is determined by the density and distribution of molecular binding among its components. Whereas, elongation at break (EB) represents film softness and elasticity, which is positively related to the flexibility and elasticity of the film. Compared to film PCA (14.43 Mpa; 50.89 %), film CS-PCA/TA-PCA exhibited significant increase in TS and EB (16.65 and 17.97 Mpa; 67.46 % and 69.83 %) (Table 1). The generation of new hydrogen bonds could account for the increased TS and EB value, which might promote the interactions of film components, thus, strengthened film resistance (Liu et al., 2022). Comparable increases in TS and EB were noted in PVA/HPMC-based film loaded roselle anthocyanin co-pigmented with oxalic acid (Huang et al., 2023). Increased EB was also reported in the sodium alginate/konjac glucomannan film incorporating *Lycium ruthenicum* anthocyanins as an indicator and tea polyphenols as a copigment (S. Wang, Li, Han, Zhuang, & Zhu, 2023).

The formation of free radicals might cause lipid and protein oxidation, promoting food quality deterioration. Hence the antioxidative activity of packing materials was of interest. In Fig. 4c, the three films showed similar free radicals scavenging capability with a DPPH scavenging rate higher than 53 %, which was attributed to the antioxidant effect of anthocyanins by capturing free radicals and blocking free radical chain reactions (Rawdkuen, Faseha, Benjakul, & Kaewprachu, 2020).

3.4. Film color response to pH

Fig. 5 displayed the relevant color parameters (L, a*, b, and ΔE) together with the pH response of PCA, CS-PCA, and TA-PCA film over the pH range of 2–11. Different colors were observed in film PCA, CS-PCA and TA-PCA. Briefly, the structure of anthocyanins presents as red flavylium cations during acidic condition. As the pH increased, anthocyanin's structure converted to colorless carbinol pseudo group bases. And when under alkaline conditions, they became blue quinoidal base (Sadi & Ferfera-Harrar, 2023; Tang et al., 2019). In Fig. 5A, all films had similar color change tendency from red-purple to blue-green, but different colors under one certain pH value. Color of PCA film changed from pinkish-purple (pH = 2) to greyish-purple (pH = 4–7), blue-green (pH = 8–9) and finally to green (pH = 10–11). While the CS-PCA film change pink to light greyish-purple (pH = 2–6), blue-green (pH = 7) and finally to green (pH = 10–11). TA-PCA film fade from pinkish-purple (pH = 2–6) to bluish-purple (pH = 7–8) and finally to greenish (pH = 10–11). Thus, CS-PCA and TA-PCA film exhibited considerable color change in the pH 2–11 range, indicating great sensitivity and pH responsiveness. Moreover, protein decomposition and degeneration in most aquatic products within a roughly pH range of 6 to 8. (R. Hao, Roy, Pan, Shah, & Mráz, 2021). As shown in Fig. 5A, the CS-PCA and TA-PCA films' color changes under pH range of 6 to 8 were clearly visible to naked eye, which indicated the films could be utilized to track the spoilage of aquatic products and monitor fish freshness.

In Fig. 5B, it is evident that b value climbed while L and a* value declined as pH increased, suggesting more noticeable greenness and

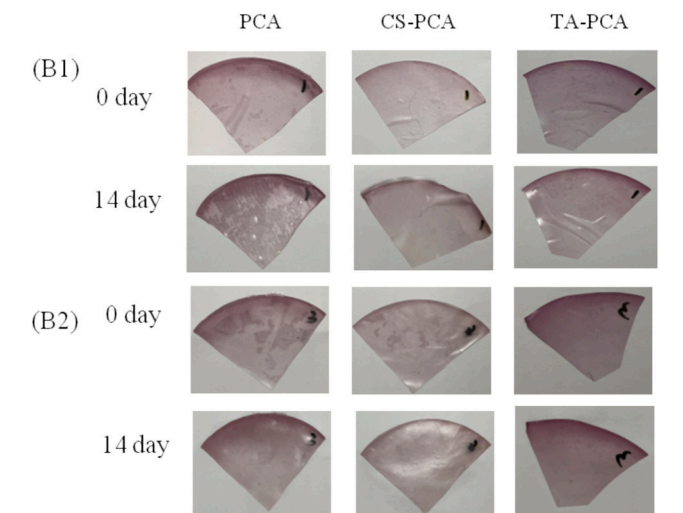
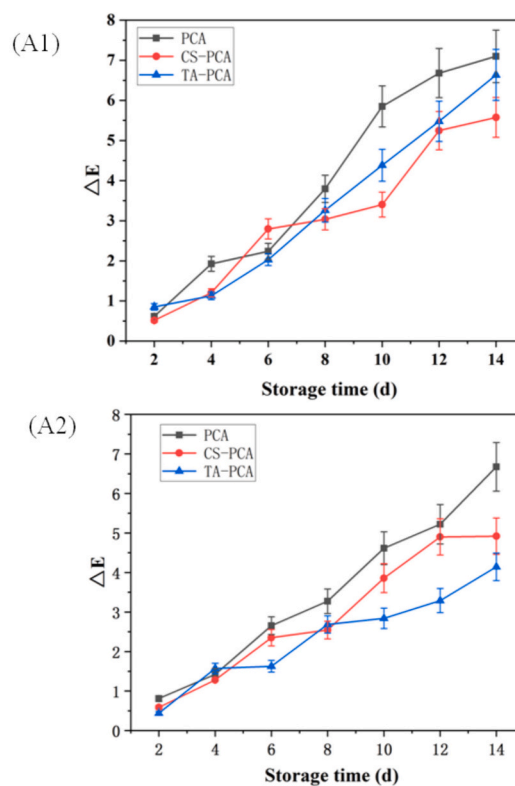


Fig. 6. The color changes of PCA, CS-PCA, TA-PCA films during 14 days at room temperature with (A1) or without (A2) an incidence of lighting. The color changes of PCA, CS-PCA, TA-PCA films during 14 days at room temperature with (B1) or without (B2) an incidence of lighting. Abbreviations see Fig. 1.

yellowness, consistent with the visual changes of films. Notably, ΔE value varied dramatically with pH in film PCA, CS-PCA and TA-PCA (ΔE variations of 5.61, 8.34, and 7.4). According to D. Liu et al. (2022), visual detectable color variation range for sensor is defined as ΔE value ≥ 5 . Consistent with the results observed by naked eye, film CS-PCA and TA-PCA showed greater variations in color parameters compared to film PCA.

3.5. Film stability

The stability of anthocyanin was influenced by a number of variables, including light and temperature, leading to insensitive and unstable indication, which greatly limits their application in food

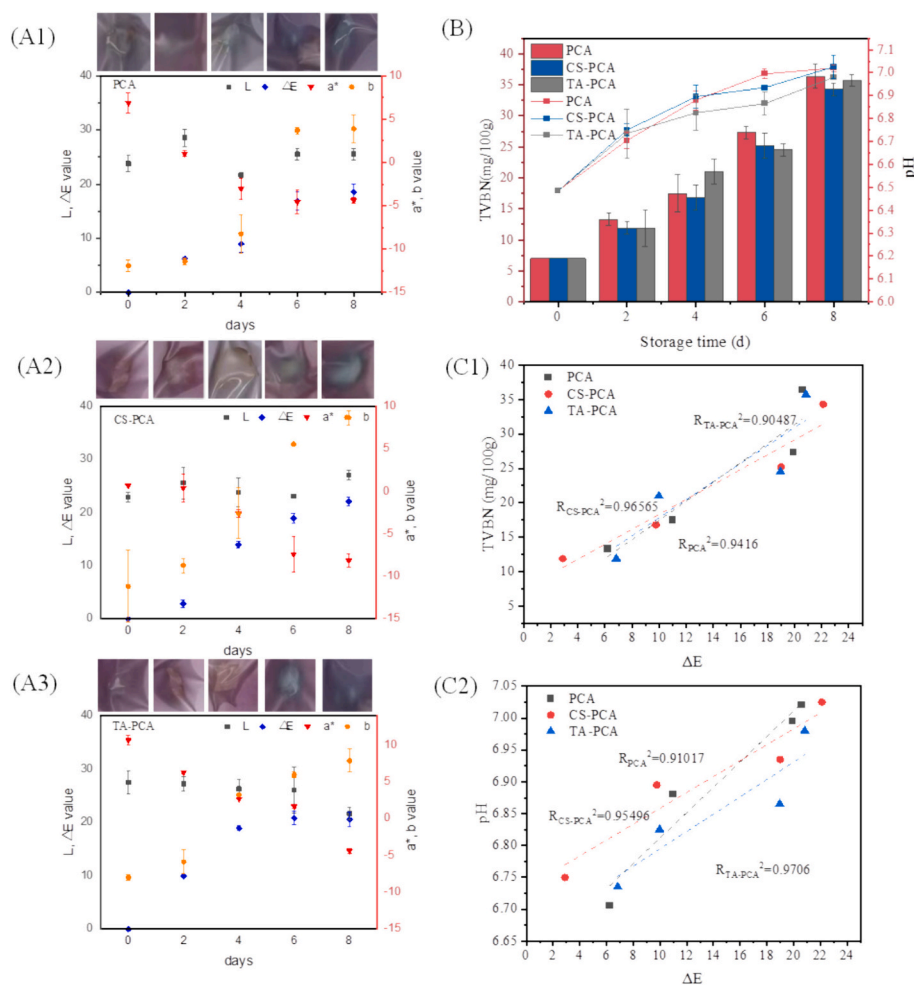


Fig. 7. Appearance and color properties of the film packing fish during storage (A1-A3); TVBN and pH of fish fillet packed with PCA, CS-PCA, TA-PCA films during chilled storage (B); correlations between ΔE and TVBN (C1) or pH (C2).

packaging (He et al., 2022). Therefore, an assessment of the color stability of intelligent film was warranted. This study evaluated the color stability of intelligent film stored at room temperature under light and dark conditions. Overall, it appeared that ΔE value of three films changed less in dark than in light (Fig. 6 A1-A2). Moreover, intelligent films show improved color stability when kept in dark. When stored in dark for 14 days, ΔE changes were 6.67 for film PCA, 4.91 for film CS-PCA and 4.14 for film TA-PCA, while 7.09, 5.57, 6.63 for them at light conditions. That is to say, the ΔE changes for CS-PCA and TA-PCA film were less than those for PCA film, which might be attributed to the generation of new hydrogen bonds between CS/TA and PCA, which improves the stability of PCA during storage (Chenjing Xie et al., 2020; S. Liu et al., 2019b). Wu and Li (2022) documented the binding of CS or TA to anthocyanins was more effective in protecting anthocyanin color stability compared to apply anthocyanins directly. The results show that film CS-PCA and TA-PCA could maintain good color stability and work well as indicator of intelligent film.

3.6. The application of the films in fish fillets freshness monitoring

Protein would break down into amino acids, resulting in the release of volatile base nitrogen (TVBN) including ammonia and various volatile amines, leading to the raise of pH value and changes the color of the intelligent film. In Fig. 7B, the TVBN value of fish fillets packed with film PCA, CS-PCA and TA-PCA increased from 7.12 mg/100 g to 16.8–21.2 mg/100 g, reaching the start point of spoilage on day 4. Meanwhile, the pH values increased from 6.48 to 6.83–6.92. Correspondingly, film PCA,

CS-PCA and TA-PCA changed from light purplish to light blue-green, rose-red to cream, dark rose to beige, with the AE value of 8.7, 15.8 and 17.1, respectively (Fig. 7A1-A3). All ΔE values were above the visible limit ($\Delta E \geq 5$), indicating that the film color variances could be observed by naked eyes. Color of all three group films turned into green since 6th day. Notably, ΔE of CS-PCA and TA-PCA film (19.8 and 21.1) were larger than ones of PCA film (15.7), suggesting that the color differentiation were more distinctive in CS-PCA and TA-PCA film, corresponding to the significant color changes observed with naked eyes. There are several types of intelligent pH indicator film developed for monitoring aquatic products quality recently (Narayanan Gopika, Radhakrishnan, Baiju, & MubeenaS, 2023; Sadi & Ferfera-Harrar, 2023; Tavassoli et al., 2023). However, the changes in color of these film themselves during storage were not quite easy to be recognized by the naked eyes, which is not conducive to the rapid and intuitive identifying of the freshness of products. Copigment-indicators, CS-PCA and TA-PCA, in this study could clearly show the quality of fish fillets (from pink to green). This implies that CS-PCA and TA-PCA films have the potential to be developed as high indication sensitive films for tracking the freshness of fish fillets.

The correlations between ΔE of all three films and TVBN, pH of fish fillets during storage at 4 °C were estimated (Fig. 7 C1 and C2). The TVBN of fish fillets was closely correlated with the AE of all three films ($R^2 = 0.90487$ – 0.96565 , Fig. 7 C1). In addition, a highly positive correlation was found between pH and AE of all three films ($R^2 = 0.91017$ – 0.97060 , Fig. 7 C2). These showed that all three films were a reliable predictor of fish fillet deterioration and were appropriate freshness indicator films

for monitoring fish fillet deterioration. Notably, the correlation of ΔE with TVBN and pH was higher for the CS-PCA and TA-PCA films than for the PCA film. The aforementioned results suggested that because of their high sensitivity and capacity for color discrimination, CS-PCA, and TA-PCA films had a higher potential for use in fish freshness identification.

4. Conclusions

Highly stable and indication-sensitive intelligent films were developed by using gelatin as matrix and anthocyanins co-pigmented with CS/TA as indicators. The co-pigmentation of PCA via CS/TA improved its stability and made its color changes under different pH conditions much easier to be distinguished by naked eye. New hydrogen bonds between CS/TA and PCA, CS-PCA/TA-PCA and gelatin were confirmed to be formed as hypothesis, which could enhance film network. Co-pigmentation of PCA with CS/TA enhanced the mechanical characteristics of film. CS-PCA and TA-PCA films showed distinct color transitions (rose-red→cream/beige→green) for chilled fish fillets during storage. Thus, the stability and quality monitoring role of PCA can be improved by CS/TA co-pigmentation, and the modified PCAs can be used to develop intelligent films with good freshness-indicating function for fish. Future work focusing on improving the precision of indicating range to improve film monitoring accuracy by modifying PCA with better co-pigmentation strategy would be interest.

CRedit authorship contribution statement

Ruoyi Hao: Writing – original draft, Investigation, Funding acquisition, Formal analysis. **Shiwen Pang:** Writing – review & editing, Investigation, Data curation. **Jan Mráz:** Writing – review & editing. **Yeye Geng:** Writing – review & editing. **Yanqiu Liu:** Writing – review & editing. **Jinfeng Pan:** Writing – review & editing, Methodology.

Declaration of competing interest

The authors declare that they have no known competing financial interests or personal relationships that could have appeared to influence the work reported in this paper.

Data availability

Data will be made available on request.

Acknowledgement

The authors were financially supported by the Grant Agency of Beihua University (Grant No. 160323501). The authors gratefully acknowledge the help of anonymous reviewers for improving this article.

Appendix A. Supplementary data

Supplementary data to this article can be found online at <https://doi.org/10.1016/j.fochx.2024.101779>.

References

- Baldwin, A., & Booth, B. W. (2022). Biomedical applications of tannic acid. *Journal of Biomaterials Applications*. <https://doi.org/10.1177/08853282211058099>
- Bao, Y., Cui, H., Tian, J., Ding, Y., Tian, Q., Zhang, W., ... Li, B. (2022). Novel pH sensitivity and colorimetry-enhanced anthocyanin indicator films by chondroitin sulfate co-pigmentation for shrimp freshness monitoring. *Food Control*, 131, Article 108441. <https://doi.org/10.1016/j.foodcont.2021.108441>
- Chen, K., Li, J., Li, L., Wang, Y., Qin, Y., & Chen, H. (2023). A pH indicator film based on sodium alginate/gelatin and plum peel extract for monitoring the freshness of chicken. *Food Bioscience*, 53, Article 102584. <https://doi.org/10.1016/j.fbio.2023.102584>

- Chenjing Xie, Q. W., Ying, R., Wang, Y., Wang, Z., & Huang, M. (2020). Binding a chondroitin sulfate-based nanocomplex with kappa-carrageenan to enhance the stability of anthocyanins. *Food Hydrocolloids*. <https://doi.org/10.1016/j.foodhyd.2019.10544>
- Ebrahimi Tirtashi, F., Moradi, M., Tajik, H., Forough, M., Ezati, P., & Kuswandi, B. (2019). Cellulose/chitosan pH-responsive indicator incorporated with carrot anthocyanins for intelligent food packaging. *International Journal of Biological Macromolecules*, 136, 920–926. <https://doi.org/10.1016/j.ijbiomac.2019.06.148>
- Etxabide, A., Maté, J. I., & Kilmartin, P. A. (2021). Effect of curcumin, betanin and anthocyanin containing colourants addition on gelatin films properties for intelligent films development. *Food Hydrocolloids*, 115, Article 106593. <https://doi.org/10.1016/j.foodhyd.2021.106593>
- Hao, R., Liu, Y., Sun, L., Xia, L., Jia, H., Li, Q., & Pan, J. (2017). Sodium alginate coating with plant extract affected microbial communities, biogenic amine formation and quality properties of abalone (*Haliotis discus hannai* Ino) during chill storage. *LWT - Food Science and Technology*, 81, 1–9. <https://doi.org/10.1016/j.lwt.2017.03.031>
- Hao, R., Roy, K., Pan, J. F., Shah, B. R., & Mráz, J. (2021). Critical review on the use of essential oils against spoilage in chilled stored fish: A quantitative meta-analysis. *Trends in Food Science & Technology*, 111, 175–190. <https://doi.org/10.1016/j.tifs.2021.02.054>
- Hao, R. Y., Pan, J. F., Khalili Tilami, S., Shah, B. R., & Mráz, J. (2020). Post-mortem quality changes of common carp (*Cyprinus carpio*) during chilled storage from two culture systems. *Journal of the Science of Food and Agriculture*, 101(n/a), 91–100. <https://doi.org/10.1002/jsfa.10618>
- He, Y., Lu, L., Lin, Y., Li, R., Yuan, Y., Lu, X., ... Li, J. (2022). Intelligent pH-sensing film based on polyvinyl alcohol/cellulose nanocrystal with purple cabbage anthocyanins for visually monitoring shrimp freshness. *International Journal of Biological Macromolecules*. <https://doi.org/10.1016/j.ijbiomac.2022.07.194>
- Huang, J., Hu, Z., Li, G., Chin, Y., Pei, Z., Yao, Q., ... Hu, Y. (2023). The highly stable indicator film incorporating roselle anthocyanin co-pigmented with oxalic acid: Preparation, characterization and freshness monitoring application. *Food Research International*, 173, Article 113416. <https://doi.org/10.1016/j.foodres.2023.113416>
- Kang, S., Wang, H., Xia, L., Chen, M., Li, L., Cheng, J., ... Jiang, S. (2020). Colorimetric film based on polyvinyl alcohol/okra mucilage polysaccharide incorporated with rose anthocyanins for shrimp freshness monitoring. *Carbohydrate Polymers*, 229, Article 115402. <https://doi.org/10.1016/j.carbpol.2019.115402>
- Li, R., Feng, H., Wang, S., Zhuang, D., & Zhu, J. (2024). A colorimetry-enhanced tri-functional film with high stability by polyphenol-anthocyanin co-pigmentation/conjugate: New prospect for active intelligent food packaging. *Food Chemistry*, 447, Article 138927. <https://doi.org/10.1016/j.foodchem.2024.138927>
- Li, R., Wang, S., Feng, H., Zhuang, D., & Zhu, J. (2024). An intelligent chitosan/gelatin film via improving the anthocyanin-induced color recognition accuracy for beef freshness differentiation monitoring. *Food Hydrocolloids*, 146, Article 109219. <https://doi.org/10.1016/j.foodhyd.2023.109219>
- Liang, T., Sun, G., Cao, L., Li, J., & Wang, L. (2019). A pH and NH₃ sensing intelligent film based on Artemisia sphaerocephala Krassch. gum and red cabbage anthocyanins anchored by carboxymethyl cellulose sodium added as a host complex. *Food Hydrocolloids*, 87, 858–868. <https://doi.org/10.1016/j.foodhyd.2018.08.028>
- Liu, D., Zhang, C., Pu, Y., Chen, S., Li, H., & Zhong, Y. (2022). Novel colorimetric films based on polyvinyl alcohol/sodium carboxymethyl cellulose doped with anthocyanins and betacyanins to monitor pork freshness. *Food Chemistry*. <https://doi.org/10.1016/j.foodchem.2022.134426>
- Liu, S., Li, S., Lin, G., Markkinen, N., Yang, H., Zhu, B., & Zhang, B. (2019a). Anthocyanin pigmentation and color attributes of bog bilberry syrup wine during bottle aging: Effect of tannic acid and gallic acid extracted from Chinese gallnut. *Journal of Food Processing and Preservation*, 43(8), Article e14041. <https://doi.org/10.1111/jfpp.14041>
- Liu, S., Li, S., Lin, G., Markkinen, N., Yang, H., Zhu, B., & Zhang, B. (2019b). Anthocyanin pigmentation and color attributes of bog bilberry syrup wine during bottle aging: Effect of tannic acid and gallic acid extracted from Chinese gallnut. *Journal of Food Processing & Preservation*. <https://doi.org/10.1111/jfpp.14041>
- Liu, Y., Ma, Y., Liu, Y., Zhang, J., Hossen, M. A., Sameen, D. E., ... Qin, W. (2022). Fabrication and characterization of pH-responsive intelligent films based on carboxymethyl cellulose and gelatin/curcumin/chitosan hybrid microcapsules for pork quality monitoring. *Food Hydrocolloids*, 124. <https://doi.org/10.1016/j.foodhyd.2021.107224>
- Lu, M., Zhou, Q., Yu, H., Chen, X., & Yuan, G. (2022). Colorimetric indicator based on chitosan/gelatin with nano-ZnO and black peanut seed coat anthocyanins for application in intelligent packaging. *Food Research International*, 160, Article 111664. <https://doi.org/10.1016/j.foodres.2022.111664>
- Nam, S., French, A. D., Condon, B. D., & Concha, M. J. C. P. (2016). Segal crystallinity index revisited by the simulation of X-ray diffraction patterns of cotton cellulose Iβ and cellulose II. *Carbohydrate Polymers*, 135, 1–9.
- Narayanan Gopika, P., Radhakrishnan, P., Baiju, P., & Mubeena, S. A. (2023). Fabrication of butterfly pea flower anthocyanin-incorporated colorimetric Indicator film based on gelatin/pectin for monitoring fish freshness. *Food Hydrocolloids for Health*. , Article 100159. <https://doi.org/10.1016/j.fhfh.2023.100159>
- Pan, J. F., Lian, H. L., Shang, M. J., Jin, W. G., Hao, R. Y., Ning, Y., ... Tang, Y. (2020). Physicochemical properties of Chinese giant salamander (*Andrias davidianus*) skin gelatin as affected by extraction temperature and in comparison with fish and bovine gelatin. *Journal of Food Measurement and Characterization*, 14, 2656–2666. <https://doi.org/10.1007/s11694-020-00512-2>
- Pang, S., Wang, Y., Jia, H., Hao, R., Jan, M., Li, S., ... Pan, J. (2023). The properties of pH-responsive gelatin-based intelligent film as affected by ultrasound power and purple cabbage anthocyanin dose. *International Journal of Biological Macromolecules*, 230, Article 123156. <https://doi.org/10.1016/j.ijbiomac.2023.123156>

- Qin, Y., Yun, D., Xu, F., Chen, D., Kan, J., & Liu, J. (2021). Smart packaging films based on starch/polyvinyl alcohol and Lycium ruthenicum anthocyanins-loaded nano-complexes: Functionality, stability and application. *Food Hydrocolloids*, 119, Article 106850. <https://doi.org/10.1016/j.foodhyd.2021.106850>
- Rawdkuen, S., Faseha, A., Benjakul, S., & Kaewprachu, P. (2020). Application of anthocyanin as a color indicator in gelatin films. *Food Bioscience*, 36, Article 100603. <https://doi.org/10.1016/j.fbio.2020.100603>
- Riahi, Z., Khan, A., Rhim, J.-W., Shin, G. H., & Kim, J. T. (2023). Gelatin/poly(vinyl alcohol)-based dual functional composite films integrated with metal-organic frameworks and anthocyanin for active and intelligent food packaging. *International Journal of Biological Macromolecules*, 249, Article 126040. <https://doi.org/10.1016/j.ijbiomac.2023.126040>
- Sadi, A., & Ferfera-Harrar, H. (2023). Cross-linked CMC/gelatin bio-nanocomposite films with organoclay, red cabbage anthocyanins and pistacia leaves extract as active intelligent food packaging: Colorimetric pH indication, antimicrobial/antioxidant properties, and shrimp spoilage tests. *International Journal of Biological Macromolecules*, 242, Article 124964. <https://doi.org/10.1016/j.ijbiomac.2023.124964>
- Susanti, I., Wijaya, H., Hasanah, F., & Heryani, S. (2018). Copigmentation of anthocyanin extract of purple sweet potatoes (*Ipomea Batatas* L.) using Ferulic acid and tannic acid. *IOP Conference Series: Earth and Environmental Science*. <https://doi.org/10.1088/1755-1315/116/1/012006>
- Tan, C., Selig, M. J., & Abbaspourrad, A. (2018). Anthocyanin stabilization by chitosan-chondroitin sulfate polyelectrolyte complexation integrating catechin copigmentation. *Carbohydrate Polymers*, 181, 124–131. <https://doi.org/10.1016/j.carbpol.2017.10.034>
- Tang, B., He, Y., Liu, J., Zhang, J., Li, J., Zhou, J., ... Wang, X. (2019). Kinetic investigation into pH-dependent color of anthocyanin and its sensing performance. *Dyes and Pigments*, 170, Article 107643. <https://doi.org/10.1016/j.dyepig.2019.107643>
- Tavassoli, M., Khezerlou, A., Firoozy, S., Ehsani, A., & Punia Bangar, S. (2023). Chitosan-based film incorporated with anthocyanins of red poppy (*Papaver rhoeas* L.) as a colorimetric sensor for the detection of shrimp freshness. *International Journal of Food Science & Technology*, 58(6), 3050–3057. <https://doi.org/10.1111/ijfs.16432>
- Wang, F., Xie, C., Tang, H., Hao, W., Wu, J., Sun, Y., ... Jiang, L. (2023). Development, characterization and application of intelligent/active packaging of chitosan/chitin nanofibers films containing eggplant anthocyanins. *Food Hydrocolloids*, 139, Article 108496. <https://doi.org/10.1016/j.foodhyd.2023.108496>
- Wang, S., Li, R., Han, M., Zhuang, D., & Zhu, J. (2023). Intelligent active films of sodium alginate and konjac glucomannan mixed by Lycium ruthenicum anthocyanins and tea polyphenols for milk preservation and freshness monitoring. *International Journal of Biological Macromolecules*, 253, Article 126674. <https://doi.org/10.1016/j.ijbiomac.2023.126674>
- Wang, Y., Zhang, J., & Zhang, L. (2022). An active and pH-responsive film developed by sodium carboxymethyl cellulose/polyvinyl alcohol doped with rose anthocyanin extracts. *Food Chemistry*, 373, Article 131367. <https://doi.org/10.1016/j.foodchem.2021.131367>
- Wu, Y., & Li, C. (2022). A smart film incorporating anthocyanins and tea polyphenols into sodium carboxymethyl cellulose/polyvinyl alcohol for application in mirror carp. *International Journal of Biological Macromolecules*, 223, 404–417. <https://doi.org/10.1016/j.ijbiomac.2022.10.282>
- Xu, M., Fang, D., Kimatu, B. M., Lyu, L., Wu, W., Cao, F., & Li, W. (2024). Recent advances in anthocyanin-based films and its application in sustainable intelligent food packaging: A review. *Food Control*, 162, Article 110431. <https://doi.org/10.1016/j.foodcont.2024.110431>
- You, Y., Li, N., Han, X., Guo, J., Zhao, Y., Huang, W., & Zhan, J. (2019). The effects of six phenolic acids and tannic acid on colour stability and the anthocyanin content of mulberry juice during refrigerated storage. *International Journal of Food Science and Technology*. <https://doi.org/10.1111/ijfs.14121>
- Zhao, S., Jia, R., Yang, J., Dai, L., Ji, N., Xiong, L., & Sun, Q. (2022). Development of chitosan/tannic acid/corn starch multifunctional bilayer smart films as pH-responsive actuators and for fruit preservation. *International Journal of Biological Macromolecules*, 205, 419–429. <https://doi.org/10.1016/j.ijbiomac.2022.02.101>